

Pharmaceutical organogels prepared from aromatic amino acid derivatives†

Guillaume Bastiat^a and Jean-Christophe Leroux^{a,b}

^aCanada Research Chair in Drug Delivery, Faculty of Pharmacy, University of Montreal, P.O. Box 6128, Downtown Station, Montreal, QC, Canada H3C 3J7

^bInstitute of Pharmaceutical Sciences, Department of Chemistry and Applied Biosciences, ETH Zürich, Switzerland. Fax: +41 (0) 44 633 1314; Tel: +41 (0) 44 633 7310

Abstract

Organogels are semi-solid systems in which an organic liquid phase is immobilized by a 3-dimensional network composed of self-assembled gelator molecules. Although there is a large variety of organogel systems, relatively few have been investigated in the field of drug delivery, owing mostly to the lack of information on their biocompatibility and toxicity. In this work, organogelator-biocompatible structures based on aromatic amino acids, namely, tyrosine, tryptophan, and phenylalanine were synthesized by derivatization with aliphatic chains. Their ability to gel an injectable vegetable oil (*i.e.* safflower oil) and to sustain the release of a model anti-Alzheimer drug (*i.e.* rivastigmine) was then evaluated. Organogels and molecular packing were characterized by differential scanning calorimetry, rheology analysis, Fourier-transform infrared spectroscopy and X-ray crystallography. The amino acid derivatives were able to gel safflower oil through van der Waals interactions and H-bonds. Tyrosine-derivatives produced the strongest gels while tryptophan was associated with poor gelling properties. The superior gelling ability of tyrosine derivatives could be explained by their well-structured 2-dimensional packing in the network. The addition of an optimal *N*-methyl-2-pyrrolidone amount to tyrosine gels fluidized the network and allowed their injection through conventional needles. Upon contact with an aqueous medium, the gels formed *in situ* and released entrapped rivastigmine in a sustained fashion.

Introduction

In situ forming implants have been extensively investigated in the pharmaceutical field for the sustained delivery of drugs *via* the parenteral route.^{1,2} So far, mainly polymeric systems have been investigated for such an application. *In situ*-forming polymeric implants can be essentially classified as solvent-free matrices³ and gels.⁴ The first category includes implants that are obtained by precipitation of a biodegradable polymer upon diffusion of a

†Electronic supplementary information (ESI) available: ¹H NMR spectrum of SPheOCH₃; ORTEP views of STyrOCH₃ and SPheOCH₃; thermograms of STyrOCH₃; thermal evolution of FTIR spectra of SPheOCH₃, STyrOCH₃ and LTyrOCH₃ and graph of *in vitro* release of RHT from SAAlaOCH₃ gels. CCDC reference numbers 713907 and 713908. For ESI and crystallographic data in CIF or other electronic format see DOI: 10.1039/b822657a

Correspondence to: Jean-Christophe Leroux.

biocompatible organic solvent in the interstitial space. These systems are now used in the clinic for the delivery of peptides for periods spanning several months.⁵ The second category mainly consists of injectable implants that are obtained by gelation of a polymeric aqueous solution upon a change in the surrounding environment (*e.g.* ionic strength, pH, temperature) or upon the application of an external stimulus (*e.g.* UV light). *In situ*-forming hydrogels are well-suited for the delivery of macromolecular labile drugs but are generally characterized by an important burst and fast release kinetics for low molecular weight drugs.⁶

More recently, a new kind of implant called an organogel, has been developed. Organogelators are low molecular weight molecules that have the ability to self-assemble in some organic solvents and trigger gel formation. The key parameters for the gelation process are the interaction forces between the organogelator molecules. Usually consisting of H-bonds, electrostatic and van der Waals interactions, they are responsible for the network formation that immobilizes solvent molecules.^{2,7} Numerous organogel systems with various properties have been described in the past few years, especially in the field of molecular photonics.⁸ Surprisingly, only a few of them have been investigated in the biomedical sciences.^{2,9} They mainly deal with the transdermal/transmucosal delivery of drugs¹⁰ and the development of injectable parenteral dosage forms.^{11–15} For example, Gao *et al.*, created a subcutaneously-injectable and biodegradable organogel based on glyceryl ester fatty acid in vegetable oil for the controlled release of levonorgestrel and ethinyl estradiol, 2 contraceptive steroids.¹¹ They showed that the oestrous cycle of female rats could be blocked for up to 40 days. Among the reasons for the limited use of organogels in medicine are the lack of data about the biocompatibility of organogelating molecules as well as the toxicity of the organic solvents employed in the preparation of the gels.

One approach to minimize the risks of toxicity is to synthesize organogelators with innocuous molecules, such as fatty acids and amino acids. Indeed, several studies have shown that amino acids and peptides derivatized with aliphatic chains could efficiently gel organic solvents.^{16–21} In addition, it is important to harness solvents with a proven safety track record, such as triglyceride oils. Over the past 5 years, our group has designed, characterized and evaluated *in situ*-forming organogels based on alkyl L-alanine alkyl esters and safflower oil.¹² The formulations were rendered injectable by the addition of a small amount of a biocompatible, water-soluble solvent which prevented complete gelation. Upon subcutaneous injection and diffusion of the gelation inhibitor, gels formed *in situ*.¹³ The resulting implants were well tolerated in rats, inducing only a mild, chronic inflammatory response.¹² Plourde *et al.* reported that leuprolide, a luteinizing hormone-releasing hormone agonist used in prostate cancer, could be released from the gels for 14 to 25 days, depending on the nature of the L-alanine (Ala) derivative included.¹⁴ This caused chemical castration lasting up to 50 days for the optimized formulation. More recently, the same organogel was used in the sustained delivery of rivastigmine, a cholinesterase inhibitor administered in the treatment of Alzheimer's disease.¹⁵

Despite these promising preliminary data, it was found that Ala derivatives produce relatively weak gels in most vegetable oils, calling for more efficient amino acid-based organogelators. In the present work, 3 aromatic amino acids, *i.e.* phenylalanine (Phe), tryptophan (Trp) and tyrosine (Tyr), grafted on various aliphatic chains, namely, lauroyl (L,

C₁₂), stearoyl (S, C₁₈) and behenoyl (B, C₂₂), were investigated for their gelling properties toward safflower oil. Compared to Ala, these amino acids possess additional interaction sites, such as an aromatic ring (Tyr, Trp, Phe), an hydroxyl function (Tyr) and an azole ring (Trp). It was hypothesized that these structural differences vs. Ala may improve network formation by introducing additional interaction loci and, therefore, generate stronger gels. Gel properties were examined by differential scanning calorimetry (DSC), rheology analysis and Fourier-transform infrared (FTIR) spectroscopy. Moreover, X-ray crystallography on single crystals was used to elucidate the organization of solid state gelator molecules in combination with the FTIR observations. A rheological method was developed to quantify the proportion of the co-solvent *N*-methyl-2-pyrrolidone (NMP), required for injection of the formulation. Finally, the release properties of various formulations, containing the anticholinesterase inhibitor rivastigmine dispersed in the gel in the solid form, were assessed *in vitro*.

Experimental

Materials

L-phenylalanine methyl ester hydrochloride, L-tyrosine methyl ester hydrochloride, L-tryptophan methyl ester hydrochloride, lauroyl chloride, stearoyl chloride, behenoyl chloride, triethylamine and *N*-methyl-2-pyrrolidone were purchased from Sigma-Aldrich Canada Ltd. (Oakville, ON, Canada) and used as received. Super-refined safflower oil (fatty acid composition of the triglycerides: 72.0% linoleic acid (C_{18:2}), 16.6% oleic acid (C_{18:1}), 7.4% palmitic acid (C_{16:0}), 2.5% stearic acid (C_{18:0}), and 1.5% *v/v* others) was kindly provided by Croda Inc. (Toronto, ON, Canada). Rivastigmine hydrogen tartrate (RHT) was purchased from LGM Pharmaceuticals Inc. (Boca Raton, FL).

Synthesis

General procedure for alkyl amino acid methyl ester synthesis—Freshly-distilled triethylamine (0.0072 mol, 2.2 eq.) was added under argon atmosphere to an anhydrous chloroform solution (100 mL) of L-amino acid methyl ester hydrochloride (0.0036 mol, 1.1 eq.). The mixture was stirred until it became clear, and was cooled to 0 °C. Then, acyl chloride (0.0033 mol, 1 eq.) dissolved in chloroform (1–2 mL) under argon atmosphere was added drop-wise. One hour after this addition phase ended, the mixture was heated to 45 °C and stirred overnight. It was successively washed with water, aqueous saturated NaHCO₃, brine, aqueous KHSO₄ (1 M), HCl (5–10%) and again with water. The organic phase was dried over MgSO₄, filtered, and concentrated under vacuum. The resulting colorless powder was recrystallized in ethyl acetate/cold hexane (4/1 *v/v*) to obtain a white powder.

Molecular weight was analyzed by LC-MSD-TOF (Agilent Technologies, Santa Clara, CA). ¹H-NMR spectra were recorded on a Bruker ARX-400 spectrometer (400 MHz, Bruker, Milton, ON, Canada) in deuterated chloroform or dimethylsulfoxide. A typical ¹H-NMR spectrum with the peak attributions is given in the ESI, Fig. S1.[†] Melting point (mp) was determined by DSC (see next section). Elemental analyses were performed with an EA1108 C, H, N, S-Analyzer from Fisons Instruments SPA (Beverly, MA).

N-stearoyl L-phenylalanine methyl ester (SPheOCH₃)—Yield: 64%; mp = 77.0 °C; Found: C 75.41, H 10.78, N 3.12. Calc. for C₂₈H₄₇O₃N: C 75.46, H 10.63, N 3.14%; δ_H (400 MHz, CDCl₃, Me₄Si, ppm): 0.88 (3 H, t, J = 8.6 Hz, (CH₂)₁₄CH₃), 1.25 (28 H, m, CH₂(CH₂)₁₄CH₃), 1.59 (2 H, m, CH₂CH₂(CH₂)₁₄), 2.17 (2 H, t, J = 9.3 Hz, COCH₂CH₂), 3.13 (2 H, m, C₆H₅CH₂CH), 3.73 (3 H, s, COOCH₃), 4.91 (1 H, dt, J = 7.6 and 10.4 Hz, CH₂CH(NH)CO), 5.85 (1 H, d, J = 10.2 Hz, NH), 7.0–7.3 (5 H, m, C₆H₅); *m/z* found: 445.2, calc. 445.68.

N-stearoyl L-tyrosine methyl ester (STyrOCH₃)—Yield: 79%; mp = 103.7 °C; Found: C 72.56, H 10.37, N 3.19. Calc. for C₂₈H₄₇O₄N: C 72.44, H 10.13, N 3.13%; δ_H (400 MHz, CDCl₃, Me₄Si, ppm): 0.88 (3 H, t, J = 6.7 Hz, (CH₂)₁₄CH₃), 1.25 (28 H, m, CH₂(CH₂)₁₄CH₃), 1.6 (2 H, qt, J = 7.3 Hz, CH₂CH₂(CH₂)₁₄), 2.17 (2 H, t, J = 7.2 Hz, COCH₂CH₂), 3.05 (2 H, m, C₆H₄CH₂CH), 3.74 (3 H, s, COOCH₃), 4.88 (1 H, dt, J = 5.8 and 7.9 Hz, CH₂CH(NH)CO), 5.61 (1 H, s, OH), 5.89 (1 H, d, J = 7.9 Hz, NH), 6.7–7.0 (4 H, m, C₆H₄); *m/z* found: 461.2, calc. 461.68.

N-stearoyl L-tryptophan methyl ester (STrpOCH₃)—Yield: 60%; mp = 73.1 °C; Found: C 73.98, H 11.00, N 5.82. Calc. for C₃₀H₄₇O₃N₂: C 74.49, H 9.79, N 5.79%; δ_H (400 MHz, CDCl₃, Me₄Si, ppm): 0.88 (3 H, t, J = 6.7 Hz, (CH₂)₁₄CH₃), 1.25 (28 H, m, CH₂(CH₂)₁₄CH₃), 1.55 (2 H, qt, 7.8 Hz, CH₂CH₂(CH₂)₁₄), 2.14 (2 H, t, J = 7.4 Hz, COCH₂CH₂), 3.33 (2 H, m, CCH₂CH), 3.7 (3 H, s, COOCH₃), 4.98 (1 H, dt, J = 5.3 and 7.9 Hz, CH₂CH(NH)CO), 5.95 (1 H, d, J = 7.7 Hz, NHCO), 7.0–7.6 (5 H, m, C₆H₄C₂H₂NH), 8.1 (1 H, m, C₆H₄C₂H₂NH); *m/z* found: 484.2, calc. 483.71.

N-lauroyl L-phenylalanine methyl ester (LPheOCH₃)—Yield: 49%; mp = 55.3 °C; Found: C 72.54, H 10.22, N 3.80. Calc. for C₂₂H₃₅O₃N: C 73.09, H 9.76, N 3.87%; δ_H (400 MHz, CDCl₃, Me₄Si, ppm): 0.85 (3 H, t, J = 8.7 Hz, (CH₂)₈CH₃), 1.23 (16 H, m, CH₂(CH₂)₈CH₃), 1.56 (2 H, m, CH₂CH₂(CH₂)₈), 2.14 (2 H, t, J = 9.6 Hz, COCH₂CH₂), 3.10 (2 H, m, C₆H₅CH₂CH), 3.71 (3 H, s, COOCH₃), 4.9 (1 H, dt, J = 7.7 and 10.4 Hz, CH₂CH(NH)CO), 5.82 (1 H, d, J = 10.4 Hz, NH), 7.0–7.3 (5 H, m, C₆H₅); *m/z* found: 361.1, calc. 361.52.

N-lauroyl L-tyrosine methyl ester (LTyrOCH₃)—Yield: 41%; mp = 86.7 °C; Found: C 68.31, H 9.30, N 3.92. Calc. for C₂₂H₃₅O₄N: C 69.99, H 9.34, N 3.71%; δ_H (400 MHz, CDCl₃, Me₄Si, ppm): 0.88 (3 H, t, J = 6.6 Hz, (CH₂)₈CH₃), 1.25 (16 H, m, CH₂(CH₂)₈CH₃), 1.58 (2 H, qt, J = 7.2 Hz, CH₂CH₂(CH₂)₈), 2.18 (2 H, t, J = 7.4 Hz, COCH₂CH₂), 3.04 (2 H, m, C₆H₄CH₂CH), 3.74 (3 H, s, COOCH₃), 4.89 (1 H, dt, J = 5.9 and 8.0 Hz, CH₂CH(NH)CO), 5.94 (1 H, d, J = 8.1 Hz, NH), 6.25 (1 H, s, OH), 6.7–6.95 (4 H, m, C₆H₄); *m/z* found: 377.1, calc. 377.52.

[†]Electronic supplementary information (ESI) available: ¹H NMR spectrum of SPheOCH₃; ORTEP views of STyrOCH₃ and SPheOCH₃; thermograms of STyrOCH₃; thermal evolution of FTIR spectra of SPheOCH₃, STrpOCH₃ and LTyrOCH₃ and graph of *in vitro* release of RHT from SALaOCH₃ gels. CCDC reference numbers 713907 and 713908. For ESI and crystallographic data in CIF or other electronic format see DOI: 10.1039/b822657a

N-behenoyl L-phenylalanine methyl ester (BPheOCH₃)—Yield: 78.5%; mp = 86.4 °C; Found: C 76.53, H 11.82, N 3.15. Calc. for C₃₂H₅₅O₃N: C 76.60, H 11.05, N 2.79%; δ_H (400 MHz, CDCl₃, Me₄Si, ppm): 0.88 (3 H, t, J = 6.6 Hz, (CH₂)₁₈CH₃), 1.25 (36 H, m, CH₂(CH₂)₁₈CH₃), 1.59 (2 H, qt, J = 6.9 Hz, CH₂CH₂(CH₂)₁₈), 2.17 (2 H, t, J = 6.6 Hz, COCH₂CH₂), 3.13 (2 H, m, C₆H₅CH₂CH), 3.74 (3 H, s, COOCH₃), 4.91 (1 H, dt, J = 5.8 and 7.8 Hz, CH₂CH(NH)CO), 5.84 (1 H, d, J = 7.4 Hz, NH), 7.0–7.3 (5 H, m, C₆H₅); *m/z* found: 501.4, calc. 501.78.

N-behenoyl L-tyrosine methyl ester (BTyrOCH₃)—Yield: 60%; mp = 106.1 °C; Found: C 74.06, H 11.50, N 2.86. Calc. for C₃₂H₅₅O₄N: C 74.23, H 10.71, N 2.71%; δ_H (400 MHz, CDCl₃, Me₄Si, ppm): 0.88 (3 H, t, J = 6.7 Hz, (CH₂)₁₈CH₃), 1.25 (36 H, m, CH₂(CH₂)₁₈CH₃), 1.57 (2 H, qt, J = 7.2 Hz, CH₂CH₂(CH₂)₁₈), 2.17 (2 H, t, J = 7.4 Hz, COCH₂CH₂), 3.05 (2 H, m, C₆H₄CH₂CH), 3.73 (3 H, s, COOCH₃), 4.87 (1 H, dt, J = 6.0 and 8.1 Hz, CH₂CH(NH)CO), 5.50 (1 H, s, OH), 5.85 (1 H, d, J = 8.2 Hz, NH), 6.7–7.0 (4 H, m, C₆H₄); *m/z* found 517.42, calc. 517.78.

General procedure for stearoyl amino acid synthesis—*N*-stearoyl L-amino acid methyl ester (SPheOCH₃, STyrOCH₃ and STrpOCH₃) were dissolved in a minimal volume of tetrahydrofuran, and adjusted to pH 10 with the addition of aqueous NaOH (1 N). The solution was stirred overnight. After acidification with HCl, the reaction mixture was extracted with chloroform and the organic phase was dried over MgSO₄, filtered, and concentrated under vacuum. The organogelator was recrystallized in ethyl acetate/cold hexane (4/1 *v/v*) to obtain a white powder.

N-stearoyl L-phenylalanine acid (SPheOH)—Yield: 89%; mp = 93.5 °C; Found: C 75.12, H 10.55, N 3.22. Calc. for C₂₇H₄₅O₃N: C 75.13, H 10.51, N 3.24%; δ_H (400 MHz, CDCl₃, Me₄Si, ppm): 0.85 (3 H, t, J = 8.6 Hz, (CH₂)₁₄CH₃), 1.23 (28 H, m, CH₂(CH₂)₁₄CH₃), 1.53 (2 H, qt, J = 9.4 Hz, CH₂CH₂(CH₂)₁₄), 2.15 (2 H, t, J = 8.3 Hz, COCH₂CH₂), 3.17 (2 H, m, C₆H₅CH₂CH), 4.85 (1 H, dt, J = 8.4 and 9.0 Hz, CH₂CH(NH)CO), 5.87 (1 H, d, J = 9.8 Hz, NH), 7.1–7.3 (6 H, m, C₆H₅ and COOH); *m/z* found: 431.2, calc. 431.65.

N-stearoyl L-tyrosine acid (STyrOH)—Yield: 79%; mp = 132.1 °C; Found: C 72.56, H 10.37, N 3.19. Calc. for C₂₇H₄₅O₄N: C 72.44, H 10.13, N 3.13%; δ_H (400 MHz, DMSO-d₆, Me₄Si, ppm): 0.85 (3 H, t, J = 6.7 Hz, (CH₂)₁₄CH₃), 1.23 (28 H, m, CH₂(CH₂)₁₄CH₃), 1.38 (2 H, qt, J = 7.2 Hz, CH₂CH₂(CH₂)₁₄), 2.03 (2 H, t, J = 7.2 Hz, COCH₂CH₂), 2.80 (2 H, m, C₆H₄CH₂CH), 4.31 (1 H, m, CH₂CH(NH)CO), 5.76 (1 H, s, OH), 6.6–7.0 (4 H, m, HOC₆H₄CH₂), 8.01 (1 H, d, J = 8.1 Hz, NH), 9.2 (1 H, s, COOH); *m/z* found: 447.2, calc. 447.65.

N-stearoyl L-tryptophan acid (STrpOH)—Yield: 67%; mp = 160.9 °C; Found: C 73.68, H 10.01, N 6.01. Calc. for C₂₉H₄₅O₃N₂: C 74.16, H 9.66, N 5.96%. δ_H (400 MHz, DMSO-d₆, Me₄Si, ppm): 0.85 (3 H, t, 6.8 Hz, (CH₂)₁₄CH₃), 1.23 (28 H, m, (CH₂)₁₄CH₃), 1.39 (2 H, qt, J = 7.1 Hz, CH₂CH₂(CH₂)₁₄), 2.04 (2 H, t, J = 6.9 Hz, COCH₂CH₂), 3.1 (2 H, m, CCH₂CH), 4.4 (1 H, m, J = 4.7 and 8.5 Hz, CH₂CH(NH)CO), 7.0–7.5 (6 H, m,

$C_6H_4C_2HNH$), 8.03 (1 H, d, $J = 7.8$ Hz, $NHCO$), 10.5 (1 H, s, $COOH$); m/z found: 470.2, calc. 469.68.

Gel preparation

The safflower oil and organogelator were mixed together at various concentrations and heated to dissolve the latter. The solution was cooled to room temperature and then stored at 4 °C during 15 h. Gelation was checked visually at room temperature by turning the sample upside down to see whether it flowed down under gravity.

DSC

Thermograms of gels were collected on a 2910 TA Instruments DSC system (New Castle, DE). The calorimeter was controlled with a Thermal Solutions (Version 1.4E) interface, and peak integration was carried out by Universal Analysis software (Version 2.5H), both from TA Instruments. The instrument was calibrated with indium. The organogelators or organogels were weighed in aluminium pans that were subsequently sealed, to establish their melting and phase transition temperatures, respectively. They were first heated at a temperature higher than their mp. Then, successive cooling and heating cycles were run between -20 °C and a temperature higher than the organogelator's mp, at a rate of 5 or 10 °C/min with a 3 min stabilization period between cycles. The organogelators' mp is given in the previous section. Gel-solution (T_{GS}) and solution-gel (T_{SG}) transition temperatures were determined by endothermic and exothermic peak maxima during the heating and cooling phases, respectively. Enthalpy values, corresponding to the area under the peaks, were also calculated.

FTIR spectroscopy

Infrared (IR) spectra of the organogelator powder were recorded on a Spectrum One FTIR spectrometer (Perkin Elmer, Shelton, CT) with a Golden Gate Diamond ATR accessory. IR spectra of the organogelators in safflower oil were recorded as a function of temperature on a Bio Rad FTS-25 spectrometer (Bio-Rad Laboratories, Randolph, MA) equipped with a water-cooled globular source, a KBr beam splitter, and a deuterated triglycine sulfate detector. Organogelator concentration was adjusted to reach a transition temperature between 20 and 70 °C. The gel was first liquefied by heating and dropped between 2 CaF_2 windows separated by a 5 μm Teflon spacer. This assembly was placed in a brass sample holder whose temperature was controlled by Peltier thermopumps. The sample was heated from room temperature to 70 °C in 5° increments. At each temperature, the sample was equilibrated for 5 min before data acquisition. Each spectrum is the average of 128 scans with a nominal resolution of 2 cm^{-1} . FTIR spectra of the organogelator in chloroform were also recorded at room temperature, with NaCl windows.

Rheology

The rheological properties of the organogels were measured in an AR2000 rheometer (TA Instruments), with parallel plate geometry (diameter of 40 mm). The organogels were heated at 80 °C and placed between the parallel plates to form a film of final thickness between 650 to 750 μm . The film was cooled to 4 °C to obtain the gel. Oscillatory strain sweeps in the γ

strain range from 0.003 to 50% at 1 Hz determined the linear regime characterized by constant dynamic moduli (storage modulus, G' , and loss modulus, G'') independent of strain amplitude. In this regime, G' and G'' were measured as a function of angular frequency (0.1 to 10 Hz) at 25 ± 0.1 °C.

X-Ray diffraction analysis

To obtain single crystals suitable for X-ray diffraction analysis, re-crystallization was performed by diffusion of a saturated hexane atmosphere into a diluted chloroform solution of organogelator. Single crystal samples were mounted on loop fiber and analyzed with a Bruker Microstar diffractometer (Bruker, Milton, ON, Canada) equipped with a platinum 135 CCD detector, Helios optics and Kappa goniometer. Structures were solved by the direct method with ShelxS-97.²² All non-H atoms were refined by full-matrix least-squares with anisotropic displacement parameters while hydrogen atoms were placed in idealized positions. The crystal-to-detector distance was 4 cm, and the data were collected in 512×512 -pixel mode. Initial unit cell parameters were quantified by least-squares fit of the angular setting of strong reflections, collected by a 10.0 degree scan in 33 frames over 3 different parts of the reciprocal space (99 frames total). One complete sphere of data was recorded. The crystal data appear below. Oak Ridge Thermal Ellipsoid Plotting (ORTEP) views and representation of the organogelators inside the crystal lattice are presented in the ESI, Fig. S2.[†]

Crystal data for *N*-stearoyl L-tyrosine methyl ester (STyr-OCH₃)—C₂₈H₄₇O₄N, $M = 461.67$ g.mol⁻¹, monoclinic, $a = 7.7988(3)$, $b = 4.9374(2)$, $c = 34.7570(14)$ Å, $\beta = 93.642(2)^\circ$, $U = 1335.63(9)$ Å³, $T = 150$ K, space group $P2_1$ (no 4), $Z = 2$, 21756 reflections measured, 4472 unique ($R_{int} = 0.040$) which were used in all calculations. The final $wR(F_2)$ was 0.1016 (all data).

Crystal data for *N*-stearoyl L-phenylalanine methyl ester (SPheOCH₃)—C₂₈H₄₇O₃N, $M = 445.67$ g.mol⁻¹, monoclinic, $a = 7.7818(4)$, $b = 4.9567(3)$, $c = 34.4265(16)$ Å, $\beta = 91.993(3)^\circ$, $U = 1327.10(12)$ Å³, $T = 150$ K, space group $P2_1$ (no 4), $Z = 2$, 21445 reflections measured, 2582 unique ($R_{int} = 0.083$) which were used in all calculations. The final $wR(F_2)$ was 0.1216 (all data).

In vitro release kinetics and high performance liquid chromatography (HPLC)

To prepare drug-loaded gels for the *in vitro* release experiments, the organogelator, rivastigine and safflower oil were weighed, mixed and heated to dissolve the organogelator. Rivastigine powder was physically dispersed in the oily solution by magnetic stirring. A small amount of NMP was added to fluidize the system. Syringes with a 20G1-gauge needle were filled with the hot dispersion (400 µL) and immediately placed on ice for 30 min. A 100-µL sample of the gels was dissolved in 1 mL of NMP, mixed with 9 mL of phosphate-buffered saline PBS (104 mM NaH₂PO₄, 36 mM NaCl, 0.1% w/v NaN₃, pH 7.4), and assayed for drug content by HPLC, as described below. 300 µL of organogels were deposited with the syringe in 50 mL of PBS at 37 °C, and stirred at 50 rpm.

Triplicate 0.5 mL samples were collected from the release medium at various time intervals and replaced by the same volume of fresh PBS. Release kinetics were measured under sink conditions. The samples collected were analyzed by HPLC. A Gilson Model 302 HPLC system (Gilson, Middletown, WI) equipped with a Gilson 234 autoinjector, a Gilson 106 pump and a Gilson 151 dual-wavelength UV-detector was employed. An Altima guard column (C18, 4.6 × 7.5 mm, 5 μm; Mandel, Guelph, ON, Canada) was placed upstream of the XTerra (RP-18, 4.6 × 250 mm, 5 μm) analytical column (Waters, Mississauga, ON, Canada). The mobile phase consisted of water/acetonitrile (78/22 v/v) with 0.1% (v/v) trifluoroacetic acid. The flow rate was set at 1 mL min⁻¹. Injection volume and detection wavelength were 20 μL and 210 nm, respectively. Each formulation was analyzed in triplicate.

Results

Ten organogelators were synthesized according to the method described previously for Ala.¹² The methyl ester amino acids (Phe, Tyr and Trp) were substituted by L, S and B aliphatic acids *via* amide links. Moreover, the 3 S organogelators were also saponified to obtain a free acid terminus. The structures of the organogelators are illustrated in Fig. 1, and the characterization data are given in the Experimental section.

Phase diagrams and transition enthalpies

T_{SG} and T_{GS} were determined by subjecting the samples to cooling and heating cycles respectively. The cooling cycle was stopped at -20 °C as it corresponded to the mp of safflower oil (data not shown). As reported earlier for Ala-based organogels¹² and other organogelling systems,^{23,24} a marked hysteretic effect was observed between T_{GS} and T_{SG} (ESI, Fig. S3[†]). T_{SG} was found to be dependent on the temperature gradient during the cooling step, since 10 °C of difference in T_{SG} was noticed between the 5 and 10 °C min⁻¹ cooling rates. The temperature gradient dependence was, however, not so pronounced for T_{GS} (<3 °C). Therefore, only T_{GS} was used to ascertain the phase transitions of the organogels (Fig. 2). The lines delimit gel-solution transition, as quantified by DSC: the dotted and solid lines correspond to situations where the gel did or did not flow, respectively, when examined at room temperature by the inverted tube method.

Fig. 2 reveals that T_{GS} depended on the nature of the amino acids. Tyr produced gels with the highest T_{GS} while the lowest T_{GS} was obtained with Phe derivatives. For instance, for an organogelator concentration of 0.15 mmol g⁻¹, the T_{GS} were 68, 57 and 45 °C for STyrOCH₃, STrpOCH₃ and SPheOCH₃, respectively. However, in the case of Trp, despite the relatively high T_{GS} value, a high concentration of organogelator was also required to prevent flow at room temperature in the inverted tube test, as demonstrated by the solid line beginning at 0.15 mmol g⁻¹ for STrpOCH₃, compared to only 0.056 mmol g⁻¹ for SPheOCH₃.

Moreover, T_{GS} was related to the length of the aliphatic chain, irrespective of the nature of the amino acid (Fig. 2). For example, for an organogelator concentration of 0.15 mmol g⁻¹, the T_{GS} was 75, 68 and 44 °C for B-, S- and LTyrOCH₃, respectively, and 55, 45 and 29 °C for B-, S- and LPheOCH₃, respectively. Increasing the length of the aliphatic chain also

decreased the concentrations required for a non-flowing gel at room temperature. They were 0.065, 0.022 and 0.019 mmol g⁻¹ for L-, S- and BTyrOCH₃, respectively, and 0.139, 0.056 and 0.05 mmol g⁻¹ for L-, S- and BPheOCH₃, respectively.

Organogelator enthalpy variations (ΔH) upon gel-solution and melting transitions were measured (Table 1). The values are related to interactions between the organogelator molecules in the gel and bulk states. Similar ΔH values were obtained in the bulk and gel states for Tyr and Trp derivatives, unlike Phe, which showed a difference of about 20 kJ mol⁻¹ between the 2 states, indicating a loss of interactions in the gel state. Organogelators with higher ΔH values gelled safflower oil at a lower concentration. At room temperature, STyrOCH₃, SPheOCH₃ and STRpOCH₃ formed gels at 0.022, 0.056 and 0.15 mmol g⁻¹ with corresponding ΔH of 61, 52 and 23 kJ mol⁻¹, respectively. The high concentration of STRpOCH₃ required to gel safflower oil could be explained by its low ΔH value, reflecting the weak associations between the organogelator molecules. Moreover, ΔH increased with aliphatic chain length, in both the gel and bulk states (Table 1). In the case of Tyr, substitution of L by B brought about a 35–40 kJ mol⁻¹ increment of ΔH .

For the acid form organogelators, only S derivatives were examined for their gelation properties. STRpOH was fully soluble at all concentrations tested and was thus not able to induce the gelation of safflower oil. STyrOH and SPheOH provided gels with high T_{GS} (e.g. 127 and 70 °C, respectively at 0.1 mmol·g⁻¹), but the corresponding ΔH values (32 and 18 kJ·mol⁻¹) were low compared to the methyl esters (52 and 61 kJ·mol⁻¹). Low ΔH values reflected weaknesses of association of the acid form in safflower oil. Indeed, these gels as well as STRpOCH₃ emulsified or disintegrated rapidly when mixed with PBS at 37 °C (data not shown). Therefore, they were not retained for further investigation as they would not make suitable parenteral implants.

Rheology

Rheological analysis was performed initially at a constant oscillation frequency of 1 Hz and variably applied strain γ . All organogels studied presented a linear regime corresponding to strain-independent storage (G') and loss moduli (G'') up to a critical γ^c value of 0.1%, beyond which G' and G'' decreased. With γ higher than 10%, G'' became greater than G' , indicating a loss of gel properties.

The mechanical properties of the organogels were then studied at 25 °C within the linear regime ($\gamma = 0.01\%$), as a function of oscillation frequency and were found to be relatively constant between 0.1 and 10 Hz (data not shown). G' and G'' profiles vs. organogel concentration are illustrated in Fig. 3, whereas Table 1 enumerates the G'/G'' values at an organogelator concentration of 0.25 mmol·g⁻¹. As already seen by DSC and the inverse tube method, the Tyr derivatives produced gels at the lowest concentrations. STyrOCH₃ gelled safflower oil at about 0.03 mmol·g⁻¹ vs. 0.06 and 0.16 mmol·g⁻¹ for SPheOCH₃ and STRpOCH₃, respectively. The poor gelling properties of STRpOCH₃ were confirmed by the lower G' and G'' values. At 0.25 mmol·g⁻¹, SPheOCH₃ had a G' value of about 1000 kPa, which is comparable to that of STyrOCH₃ (Fig. 3). However, the STyrOCH₃ gel was more elastic with a G'/G'' ratio of 8.4 compared to 4.3 for SPheOCH₃. The effect of aliphatic chain length on gelling behaviour was then investigated with Tyr and Phe derivatives. As

observed previously by DSC, an increase in alkyl chain length from S to B was associated with a decrease in gelation concentration (*e.g.* from 0.03 to 0.01 mmol·g⁻¹ for Tyr) (Fig. 3). The G'/G'' ratios did not seem to be affected by chain length and were similar for B and L Phe/Tyr organogelators (Table 1).

FTIR spectroscopy

The molecular interactions in bulk (powder), solution (organogelator in chloroform) and gel states (organogelator in safflower oil) were thus analyzed by FTIR spectroscopy to monitor H-bonds in the gelation process.^{12,15,17} Table 2 shows the position of the characteristic bands corresponding to various vibrations in the 3 states: (i) stretching vibration (sv) of OH and NH of the amide and amine groups (3300–3700 cm⁻¹), (ii) sv of carbonyl of ester (1700–1750 cm⁻¹), (iii) sv of carbonyl of the amide groups (amide I band: 1600–1700 cm⁻¹), and (iv) bending vibration (bv) of NH of the amide groups (amide II band: 1460–1550 cm⁻¹). For gels, peaks in the 1750–1700 cm⁻¹ region were not analyzed because the triglycerides of safflower oil possess ester bonds that screen the sv of the organogelator ester bond. Three organogelators, namely SPheOCH₃, STrpOCH₃ and STyrOCH₃, were characterized by FTIR to examine the impact of amino acid structure on the association mechanism.

In the case of SPheOCH₃, similar IR spectra of the bulk and gel states were obtained whereas differences in band positions were noticed in solution states. For bulk as well as gel states, the NH amide group was involved in H-bonding, as demonstrated by sv and bv peaks at 3338 and 1528/1530 cm⁻¹, respectively. These peaks appeared at 3432 and 1507 cm⁻¹ in solutions for free NH amide. Similarly, the CO amide group formed H-bonds in the bulk and gel states (sv band at 1647/1648 cm⁻¹), whereas it remained free in solution (1671 cm⁻¹). As reported in Table 2, there were no changes in the CO ester sv band in bulk and solution states. SPheOCH₃ was involved in only one type of H-bonding, between NH (donor) and CO (acceptor) of the amide group. Heating the gel up to T_{GS} led to a loss of H-bonds, as reflected by band positions at high temperature, corresponding to the characteristic signals of SPheOCH₃ in CHCl₃ solution (ESI, Fig. S4A[†]).

STrpOCH₃ displayed the same IR spectral characteristics as SPheOCH₃ in the bulk/gel *vs.* solution states with respect to shifts in NH and CO amide bands. In addition, the NH amine of theazole ring and CO of the ester group formed H-bonds in the bulk state, as manifested by the characteristic sv peak at 3367 and 1723 cm⁻¹, respectively (*vs.* 3430 and 1741 cm⁻¹ for the free amine and free carbonyl of ester in chloroform). STrpOCH₃ molecules interacted *via* H-bonds with NH amine and amide (donors) and CO ester and amide (acceptors). Here, again, upon heating, there was a progressive disruption of H-bonds and a shift of the bands to the characteristic position of the IR spectrum in chloroform (ESI, Fig. S4B[†]).

The last organogelator, STyrOCH₃, also behaved similarly in the bulk and gel states. Compared to the chloroform solution, shifts were observed for the NH amide, CO amide and OH sv bands. These functions formed H-bonds in the bulk and gel states. As with SPheOCH₃, the CO ester sv band remained relatively unaffected by the physical state of STyrOCH₃. Due to the temperature limit of the FTIR apparatus and the thermal evolution of STyrOCH₃, IR spectra could not be monitored. Therefore, the impact of temperature on IR

trace was studied using a Tyr derivative with a lower T_{GS} , namely, LTyrOCH₃ (ESI, Fig. S4C). As observed for the other organogelators, heating the gel led to a loss of H-bond association and subsequent transition to the solution state.

X-Ray diffraction analysis

In this work, X-ray diffraction was undertaken to elucidate the organization of the organogelators in the bulk state and to provide some insights into the possible molecular arrangement that may occur in the gels. STrpOCH₃ was excluded from this analysis as we did not succeed in obtaining a single crystal. Crystal structure determinations for STyrOCH₃ and SPheOCH₃ are given in the Experimental section. Structures and molecular packing were extracted, revealing the presence of the H-bonds in the system.

For STyrOCH₃, the crystal system was monoclinic. As seen in the ESI, Fig. S2B, there were 2 antiparallel organogelator molecules (with the Tyr head and the aliphatic tail in opposite directions) per lattice. Fig. 4A and 4B illustrate the molecular packing of STyrOCH₃ in the crystal. It consisted of a head-to-head structure with intercalated, anti-parallel and parallel STyrOCH₃ molecules. In these figures, the molecular packing is represented after 1-time lattice expansion along the b axis and along the b and c axes, respectively. From Fig. 4A, it can be seen that van der Waals interactions occurred between the aliphatic chains. Fig. 4A and 4B show H-bonds between the NH and CO of amide functions for 2 parallel organogelators and between the Tyr OH groups facing each other for the 2 head-to-head organogelators. The geometries of H-bonds involved in packing are reported in Table 3. These results corroborated the analysis of STyrOCH₃ interactions by FTIR spectroscopy. Interestingly, there was no π - π stacking between the aromatic Tyr moieties. The distance between the nearest centroid of the aromatic ring was 4.9 Å, which was too large for such an interaction. The aromatic rings between 2 parallel molecules were not superimposed (Fig. 4A), and were perpendicular to each other for the head-to-head molecules (Fig. 4B).

Analysis of SPheOCH₃ revealed a similar crystal system in some respects (ESI, Fig. S2D[†]). In Fig. 4C and 4D, molecular packing is represented after 1-time lattice expansion along the b axis and along the a, b and c axes, respectively. As for STyrOCH₃, van der Waals interactions between aliphatic chains were evident. As observed previously by FTIR spectroscopy, there was only 1 H-bond between the NH and CO of amide functions for 2 parallel organogelators. No π - π stacking between the aromatic Phe moieties was apparent (Fig. 4D), and assembly of the aromatic rings was similar to STyrOCH₃. They were not aligned between parallel organogelators and were perpendicular to the head-to-head molecules (Fig. 4C and 4D).

Effect of NMP on the gelation process

In the formulation of parenteral organogels, the addition of a water-soluble solvent, such as NMP, was previously demonstrated to facilitate injection by partly disrupting associations between the organogelator molecules.^{12,14,15,25} NMP is relatively innocuous and already found in FDA-approved parenteral formulations (Eligard[®]).⁵ The amount that would be used *in vivo* would be low and in a non toxic range (about 15 mg per implant, *i.e.* less than 50 mg kg⁻¹ in rats).²⁶ The proportion of NMP is important since not enough solvent may prevent

injection, whereas excess NMP could impair the gelation process *in situ*, leading to significant burst release. Therefore, the effect of NMP content on STyrOCH₃ systems was investigated by rheology analysis at various organogelator concentrations (Fig. 5, solid symbols).

At all STyrOCH₃ concentrations studied, it was found that at a molar NMP/organogelator ratio greater than 3–4, the gel lost its properties, as shown by the very low values obtained for G' (Fig. 5A) and G'/G'' (Fig. 5B). This means that about 3 molecules of NMP per organogelator molecule were required to substantially suppress network formation. In comparison, for SPheOCH₃ and STrpOCH₃, fluidization of the formulation occurred at a NMP/organogelator molar ratio of 6–7 (Fig. 5A, open symbols).

To assess injectability, formulations containing 0.2 mmol·g⁻¹ (9.2% w/w) of STyrOCH₃ and various amounts of NMP were prepared and then extruded through a 20G1 needle in PBS. At a NMP/organogelator ratio of 1, injection was difficult and gel filaments were obtained (Fig. 6A). At a critical ratio of 3 (Fig. 6B), injection was easy, and a rounded shape gel formed in PBS. In the presence of further excess NMP (NMP/STyrOCH₃ = 10), barely any resistance was encountered upon injection. However, small heterogeneous pieces of gels were evident in the dispersion medium (Fig. 6C).

***In vitro* release kinetics**

Tyr-derivatives (S- and BTyrOCH₃) were then evaluated for sustained release of the anti-Alzheimer drug RHT. In addition to the length of the fatty acid substituent (S vs. B), the impacts of organogelator concentration (0.05 vs. 0.1 mmol·g⁻¹) (2.3 vs. 4.6% and 2.6 vs. 5.2% w/w for S- and BTyrOCH₃, respectively) and molar NMP/organogelator ratio (3 vs. 6) on the release kinetics of RHT were investigated. The release kinetics were only monitored for 7 days, mainly to measure the extent of burst release upon injection of the formulations in aqueous medium. Indeed, degradation of the implants, which occurs *in vivo*, cannot be reliably replicated under *in vitro* conditions. Therefore, it is of little value to follow the release rate over a period exceeding a few days as the release rates would otherwise be largely underestimated. As shown in Fig. 7, increasing aliphatic chain length from S to B produced a significant reduction of the initial release rate at both gelator concentrations. For example, after 7 days, 13.5% of RHT was released from the STyrOCH₃ gel compared to 9% from the BTyrOCH₃ system at 0.05 mmol·g⁻¹. Similarly, augmenting organogelator concentration from 0.05 to 0.1 mmol·g⁻¹ led to a slight attenuation of immediate release. The most drastic effect was observed by changing the NMP/organogelator ratio. At a ratio of 6 and a STyrOCH₃ concentration of 0.05 mmol·g⁻¹ (2.3% w/w) a large and highly variable burst was seen (18% release within 24 h). When the ratio was decreased to 3 (*i.e.* the minimum value to ensure swift injection), the burst dropped by about 2-fold and was accompanied by less intersample variability.

Discussion

Two of the main objectives of this work were: (i) to identify organogelators that would be superior to Ala derivatives in gelling safflower oil, and (ii) to study the impact of gelator structure (nature of the amino acid and length of the aliphatic chain) on self-assembling

properties. From the DSC data and rheological analysis of the gels, it appeared that esterified Tyr-derivatives (S- and BTyrOCH₃) were endowed with the best gelling properties compared to Trp, Phe and even Ala.¹² Gels formed at low concentrations, and T_{GS} was higher than for the other derivatives (Fig. 2). At a concentration of 0.25 mmol·g⁻¹, the elastic moduli, G', and G'/G'' ratios for S- and BTyrOCH₃ were in the range of 10⁶ Pa and 8, respectively. These values, indicative of the formation of an elastic gel, are slightly greater than those reported for SAlaOCH₃ (G'/G'' = 5.6 at 0.27 mmol·g⁻¹)¹⁵ and comparable to alkylated glutamic acid gels in isostearyl alcohol and propylene glycol at higher concentration (G' = 2 · 10⁶ and G'/G'' = 10 at 49.3 mmol·g⁻¹).¹⁸ The good gelling ability of the Tyr derivatives could be directly linked to their association mechanism in safflower oil. These organogelators seemed to pack similarly in the bulk and gel states, as evidenced indirectly by the similar ΔH values (Table 1) and bands in the IR spectra (Table 2).

Self-assembly was most probably driven by van der Waals interactions between the aliphatic chains and by H-bonds between NH and CO in the amide functions (Table 2 and Fig. 4A). Safflower oil is not commonly used as solvent for organogelators but its dielectric constant (ε) should be comparable to that of other vegetable oils²⁷ (2–3 F·m⁻¹) and close to that of hexane.²⁸ In these solvents both van der Waals and H-bond interactions have often been reported as key elements in the gelation mechanism.^{19,20} Our data suggest that van der Waals interactions have an important role in the association process. Increasing the length of the aliphatic chain from stearyl (C₁₈) to behenoyl (C₂₂) resulted in the following effects: (i) a decrease of the minimal Tyr-based organogelator concentration required to induce gelation, (ii) an increase in the T_{GS}, (iii) a 20 kJ·mol⁻¹-increase of ΔH and (iv) improved rheological properties. Bhattacharya *et al.* have also shown that the stability of the network was enhanced upon increasing the aliphatic chain length of Phe-based organogelators in a mixture hexane/ethyl acetate (EtOAc) 70/30 (v/v) (ε_{EtOAc} = 6 F·m⁻¹).²⁰ Nevertheless, van der Waals interactions are not sufficient to stabilize the gel state, since the gel-solution transition was correlated with the loss of H-bonds upon increasing the temperature (ESI, Fig. S4A to S4C[†]).

A distinctive feature of Tyr-derivatives was H-bonds between the OH of phenolic moieties that stabilized the network in 2 dimensions (Table 2 and Fig. 4B). Assuming a similar organization between the bulk and gel states, the Tyr-based network can be described as an H-bonded head-to-head structure with intercalated, anti-parallel and parallel organogelator molecules stabilized by H-bonds and van der Waals interactions.

As opposed to Tyr, Trp was not an efficient gelating backbone for safflower oil. Indeed, at room temperature, about 10-fold more STrpOCH₃ than STyrOCH₃ was required to gel the safflower oil. This poor gelation ability was confirmed by rheological analysis (Fig. 3), and was reflected by the low association ΔH value (Table 1). Gelation occurred *via* van der Waals interactions and H-bonds (NH amine and amide, and CO ester and amide functions) between the organogelator molecules. DSC and IR data suggested that self-assembly followed the same pattern in the bulk and gel states. Unfortunately, it was not possible to elucidate the molecular organization of the network by X-ray diffraction analysis since a single crystal could not be generated. It is possible that for Trp derivatives, packing may not be as well organized as for the other tested gelators.

Phe-derivatives provided gels with intermediate properties between those of Tyr and Trp, and very close to SALaOCH₃ gels.¹² While their T_{GS} was lower than those of Trp and Tyr for a given aliphatic chain length (Fig. 2), intermediate values were obtained for elastic and storage moduli (Fig. 3) as well as for ΔH of association (Table 1). Interestingly, in all 3 Phe-derivatives (L, S and B) (Table 1), there was a 20 kJ·mol⁻¹ loss in ΔH from the bulk to the gel state. IR experiments revealed no differences in H-bond association between these 2 states (H-bonds between the NH and CO of amide functions) (Table 2). X-Ray diffractometry analysis showed that SPheOCH₃ packed in a similar fashion as STyrOCH₃, excluding H-bonding between the head-to-head phenolic rings. As for STyrOCH₃, the aromatic rings of 2 parallel SPheOCH₃ molecules were not involved in π - π stacking, but were close enough to interact (Fig. 4D). One can hypothesize that such interactions may be disturbed in the presence of safflower oil, resulting in a decreased ΔH value compared to the bulk compound. Bhattacharya *et al.* found through modeling that π - π stacking did not occur with another Phe-based organogelator in a mixture of hexane/EtOAc 70/30 (v/v).²⁰ Rahman *et al.* have shown that Phe modified with an aliphatic chain and another aromatic group induced the gelation of cyclohexane. The association of the organogelator in the gel was due to van der Waals interactions, H-bonds and π - π stacking between the aromatic rings of two organogelator molecules.²¹ In their system, the presence of a second aromatic ring in the vicinity of the parent one favoured π - π stacking.

To be used as injectable and *in situ*-forming implants, organogel structure needs to be fluidized to facilitate its injection through conventional needles. NMP was previously found to be a suitable agent for this purpose.¹³⁻¹⁵ Rheological analysis revealed that, in the case of STyrOCH₃, a minimum NMP/organogelator molar ratio of 3 was sufficient to inhibit gelation. This gel was more sensitive to the addition of NMP than the Phe and Trp derivatives. Since STyrOCH₃ self-assembled into a well organized network, it is possible that a small perturbation brought about by the addition of NMP was sufficient to substantially suppress the gelation process.

This minimum NMP/organogelator ratio still allows the formation of an homogenous implant after injection. A higher proportion of NMP led to fragmentation of the gel matrix in aqueous buffer. More importantly, NMP concentration was found to greatly affect the burst release of incorporated RHT. Apart from fragmenting the gel, a high NMP concentration can increase release by slowing down the gelation process and dragging the drug outside the implant as NMP diffuses in the aqueous phase. Among all organogelators investigated in this study for the sustained delivery of RHT, Tyr-derivatives, and, particularly, the S and B forms appeared to be the most appropriate compounds. In accordance with the DSC and rheological data, the lowest burst was obtained with the implant presenting the highest gelator concentration (0.1 mmol·g⁻¹ or 5.2% w/w) and longest aliphatic chain (B). Interestingly, Tyr-derivatives were far superior to our previous Ala-based systems and could be injected with less NMP. For instance, at SALaOCH₃ concentrations of 0.05 and 0.1 mmol·g⁻¹ (1.8 and 3.9% w/w) and at a NMP/organogelator ratio of 5 (optimal NMP concentration for the injection of SALaOCH₃ formulation¹³⁻¹⁵), burst releases of more than 70 and 35%, respectively, were observed (ESI, Fig. S5[†]). These values largely exceed the bursts obtained with STyrOCH₃ (Fig. 7). Gels prepared with SALaOCH₃ are not as strong and elastic as their Tyr counterparts.

Conclusion

In this work, a series of new organogelators based on different amino acids and various chain lengths have been synthesized and characterized with respect to their ability to gel safflower oil. Tyr-based gelators, and, in particular, the derivative bearing the longest chain length (BTyrOCH₃) were found to display the strongest gelation properties. Tyr organogelators probably self-assembled in the network in 2-dimensional configuration involving van der Waals interactions and H-bonds in one direction and H-bonds between the phenol heads in the other direction. Such an arrangement can be, however, easily disrupted with a relatively low concentration of NMP, allowing the injection of organogels with conventional needles. Implants prepared with BTyrOCH₃ are characterized by low-burst release and, therefore, appear to be promising systems for the sustained parenteral delivery of anti-Alzheimer drugs, such as RHT. Future work will be aimed at assessing the pharmacokinetics as well as the pharmacological activity of RHT-loaded BTyrOCH₃ implants.

Supplementary Material

Refer to Web version on PubMed Central for supplementary material.

Acknowledgments

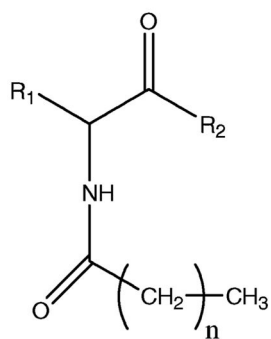
The Canadian Institutes of Health Research, the Natural Sciences and Engineering Council of Canada (Stacie Fellowship to JCL) and the Canada Research Chair program are acknowledged for their financial support. The authors thank Francine Bélanger for her invaluable help in the X-ray crystallography analyses.

References

1. Packhaeuser CB, Schnieders J, Oster CG, Kissel T. *Eur J Pharm Biopharm.* 2004; 58:445–455. [PubMed: 15296966]
2. Vintiloiu A, Leroux JC. *J Control Release.* 2008; 125(3):179–192. [PubMed: 18082283]
3. Heller J, Barr J, Ng SY, Shen HR, Schwach-Abdellaoui K, Gurny R, Vivien-Castioni N, Loup PJ, Baehni P, Mombelli A. *Biomaterials.* 2002; 23(22):4397–4404. [PubMed: 12219830] Van de Weert M, Van Stehenbergen MJ, Cleland JL, Heller J, Henning WE, Crommelin DJA. *J Pharm Sci.* 2002; 91(4):1065–1074. [PubMed: 11948545] Chu FM, Jayson M, Dineen MK, Perez R, Harkaway R, Tyler RC. *J Urol.* 2002; 168(3):1199–1203. [PubMed: 12187267]
4. Qiu B, Stefanos S, Ma J, Laloo A, Perry BA, Leibowitz MJ, Sinko PJ, Stein S. *Biomaterials.* 2002; 24(1):11–18. Cohen S, Lobel E, Trevgoda A, Peled Y. *J Control Release.* 1997; 44(2–3):201–208. Zentner GM, Rathi R, Shih C, McRea JC, Seo MH, Oh H, Rhee BG, Mestecky J, Moldoveanu Z, Morgan M, Weitman S. *J Control Release.* 2001; 72(1–3):203–215. [PubMed: 11389999]
5. Sartor O. *Urology.* 2003; 61(2 Suppl 1):25–31. [PubMed: 12667884]
6. Ruel-Gariépy E, Leroux J-C. *Eur J Pharm Biopharm.* 2004; 58(2):409–426. [PubMed: 15296964] Ruel-Gariépy E, Leclair G, Hildgen P, Gupta A, Leroux J-C. *J Control Release.* 2002; 82(2–3):373–383. [PubMed: 12175750]
7. Terech P, Weiss RG. *Chem Rev.* 1997; 97(8):3133–3159. [PubMed: 11851487]
8. Mallia VA, Tamaoki N. *Chem Soc Rev.* 2004; 33(2):76–84. [PubMed: 14767503] Ajayaghosh A, Praveen VK, Vijayakumar C. *Chem Soc Rev.* 2008; 37(1):109–122. [PubMed: 18197337]
9. Kumar R, Katare OP. *AAPS Pharm Sci Tech.* 2005; 6(2):E298–E310. Murdan S. *Expert Opin Drug Deliv.* 2005; 2(3):489–505. [PubMed: 16296770] Bonacucina G, Cespi M, Misici-Falzi M, Palmieri GF. *J Pharm Sci.* 2009; 98(1):1–42. [PubMed: 18452176]

10. Mahler P, Mahler F, Duruz H, Ramazzina M, Liguori V, Mautone G. *Drugs Exp Clin Res.* 2003; 29(1):45–52. [PubMed: 12866363] Agrawal GP, Juneja M, Agrawal S, Jain SK, Pancholi SS. *Pharmazie.* 2004; 59(3):191–193. [PubMed: 15074590] Upadhyay KK, Tiwari C, Khopade AJ, Bohidar HB, Jain SK. *Drug Dev Ind Pharm.* 2007; 33(6):617–625. [PubMed: 17613026] Pénczes T, Blazsó G, Aigner Z, Falkay G, Eros I. *Int J Pharm.* 2005; 298(1):47–54. [PubMed: 15893893] Murdan S, Gregoriadis G, Florence AT. *Eur J Pharm Sci.* 1999; 8(3):177–185. [PubMed: 10379040] Jones DS, Muldoon BC, Woolfson AD, Sanderson FD. *J Pharm Sci.* 2007; 96(10): 2632–2646. [PubMed: 17702045]
11. Gao ZH, Crowley WR, Shukla AJ, Johnson JR, Reger JF. *Pharm Res.* 1995; 12(6):864–868. [PubMed: 7667191]
12. Motulsky A, Lafleur M, Couffin-Hoarau AC, Hoarau D, Boury F, Benoit JP, Leroux JC. *Biomaterials.* 2005; 26(31):6242–6253. [PubMed: 15916802]
13. Couffin-Hoarau AC, Motulsky A, Delmas P, Leroux JC. *Pharm Res.* 2004; 21(3):454–457. [PubMed: 15070096]
14. Plourde F, Motulsky A, Couffin-Hoarau AC, Hoarau D, Ong H, Leroux JC. *J Control Release.* 2005; 108(2–3):433–441. [PubMed: 16182402]
15. Vintiloiu A, Lafleur M, Bastiat G, Leroux JC. *Pharm Res.* 2008; 25(4):845–852. [PubMed: 17694395]
16. Bhattacharya S, Acharya SNG, Raju AR. *Chem Commun.* 1996; 17:2101–2102. Hanabusa K, Tange J, Taguchi Y, Koyama T, Shirai H. *J Chem Soc, Chem Commun.* 1993; 4:390–392. Hidaka H, Murata M, Onai T. *J Chem Soc, Chem Commun.* 1984; 9:562–564. Suzuki M, Sato T, Kurose A, Shirai H, Hanabusa K. *Tetrahedron Lett.* 2005; 46(16):2741–2745. Ihara H, Yamada T, Nishihara M, Sakurai T, Takafuji M, Hachisako H, Sagawa T. *J Mol Liq.* 2004; 111(1–3):73–76. Kobayashi S, Hanabusa K, Suzuki M, Kimura M, Shirai H. *Chem Lett.* 1999; 10:1077–1078. Coates IA, Hirst AR, Smith DK. *J Org Chem.* 2007; 72:3937–3940. [PubMed: 17439286] Chow HF, Zhang J, Lo CM, Cheung SY, Wong KW. *Tetrahedron.* 2007; 63:363–373. Escuder B, Marti S, Miravet JF. *Langmuir.* 2005; 21:6776–6787. [PubMed: 16008387] Fu X, Yang Y, Wang N, Wang H, Yang Y. *J Mol Recognit.* 2007; 20(4):238–244. [PubMed: 17624913] Suzuki M, Nigawara T, Yumoto M, Kimura M, Shirai H, Hanabusa K. *Org Biomol Chem.* 2003; 1:4124–4131. [PubMed: 14664402] Ragunathan KG, Bhattacharya S. *Chem Phys Lipids.* 1995; 77(1):13–23.
17. Suzuki M, Yumoto M, Shirai H, Hanabusa K. *Chem Eur J.* 2008; 14(7):2133–2144. [PubMed: 18161708] Zhan C, Gao P, Liu M. *Chem Commun.* 2005; 4:462–464.
18. Li JL, Liu XY, Wang RY, Xiong JY. *J Phys Chem B.* 2005; 109(51):24231–24235. [PubMed: 16375418]
19. Suzuki M, Nakajima Y, Yumoto M, Kimura M, Shirai H, Hanabusa K. *Langmuir.* 2003; 19(21): 8622–8624. Suzuki M, Sato T, Kurose A, Shirai H, Hanabusa K. *Tetrahedron Lett.* 2005; 46(16): 2741–2745. Hanabusa K, Naka Y, Koyama T, Shirai H. *J Chem Soc, Chem Commun.* 1994; 23:2683–2684. Hardy JG, Hirst AR, Ashworth I, Brennan C, Smith DK. *Tetrahedron.* 2007; 63:7397–7406. Hanabusa K, Tanaka R, Suzuki M, Kimura M, Shirai H. *Adv Mater.* 1997; 9(14): 1095–1097.
20. Bhattacharya S, Acharya SNG. *Chem Mater.* 1999; 11(11):3121–3132.
21. Rahman MM, Czaun M, Takafuji M, Ihara H. *Chem Eur J.* 2008; 14(4):1312–1321. [PubMed: 18033705]
22. Flack HD. *Acta Cryst.* 1983; A39:876–881. Flack HD, Schwarzenbach D. *Acta Cryst.* 1988; A44:499–506. SAINT, Release 7.34A. Bruker AXS Inc; Madison, WI 53719-1173: 2006. Sheldrick, GM. SADABS. Bruker AXS Inc; Madison, WI 53719-1173: 1996. Sheldrick GM. *Acta Cryst.* 2008; A64:112–122. SHELXTL version 6.12. Bruker AXS Inc; Madison, WI 53719-1173: 2001. APEX2 version 2.1-0. Bruker AXS Inc; Madison, WI 53719-1173: 2006. XPREP Version 2005/2. Bruker AXS Inc; Madison, WI 53719-1173: 2005.
23. Maji SK, Malik S, Drew MGB, Nandi AK, Banerjee A. *Tetrahedron Lett.* 2003; 44(21):4103–4107.
24. Yasuda Y, Iishi E, Inada H, Shiota Y. *Chem Lett.* 1996; 25(7):575–576. Das AK, Manna S, Drew MGB, Malik S, Nandi AK, Banerjee A. *Supramol Chem.* 2006; 18(8):645–655.

25. Royals MA, Fujita SM, Yewey GL, Rodriguez J, Schultheiss PC, Dunn RL. *J Biomed Mater Res.* 1999; 45:231–239. [PubMed: 10397981]
26. Becci PL, Gephart LA, Koschier FJ, Johnson WD, Burnette LW. *J Appl Toxicol.* 1983; 3(2):83–86. [PubMed: 6886300] Saillenfait AM, Gallissot F, Langonne I, Sabate JP. *Food Chem Tox.* 2002; 40:1705–1712.
27. Rudan-Tasic D, Klofutar C. *Acta Chim Slov.* 1999; 46(4):511–521. Faktorova D. *Meas Sci Rev.* 2007; 7(2):12–15.
28. Wohlfarth, C. *Landolt-Börnstein, Numerical Data and Functional Relationships in Science and Technology, Group IV: Physical chemistry.* Lechner, MD., editor. Vol. 17. Springer; Berlin: 2008. p. 360-362.



$R_2 =$ **OCH₃** → methyl ester form
OH → acid form

$n =$ 10 → lauroyl (**L**)
 16 → stearoyl (**S**)
 20 → behenoyl (**B**)

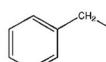
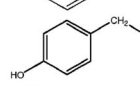
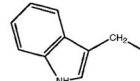
$R_1 =$  → phenylalanine (**Phe**)
 → tyrosine (**Tyr**)
 → tryptophan (**Trp**)

Fig. 1.
 Structure of the organogelators.

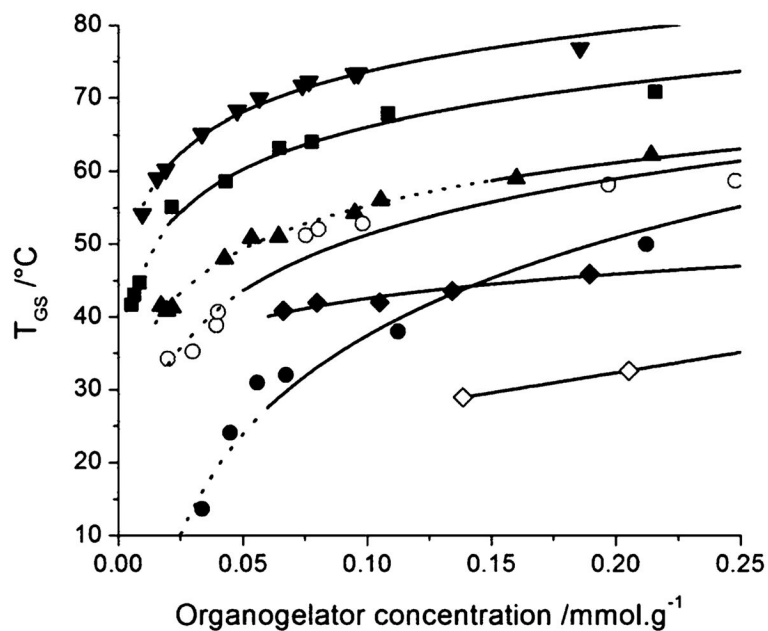


Fig. 2. Gel-solution transition temperature (T_{GS}) determined from DSC data as a function of STyrOCH₃ (■), SPhEOCH₃ (●), STrpOCH₃ (▲), BTyrOCH₃ (▼), BPhEOCH₃ (○), LTrpOCH₃ (◆) and LPhEOCH₃ (◇) concentration. Dotted lines show systems that flowed at room temperature when subjected to the inverse tube method.

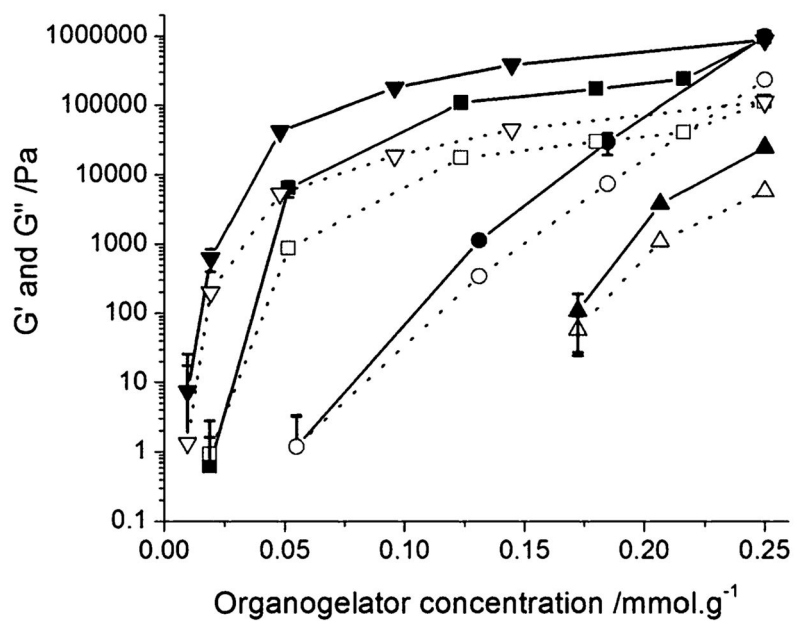


Fig. 3. Elastic (G' , closed symbols and solid lines) and viscous (G'' , open symbols and dotted lines) moduli of STyrOCH₃ (■, □), SPheOCH₃ (●, ○), STrpOCH₃ (▲, △) and BTyrOCH₃ (▼, ▽) gels in safflower oil vs. organogelator concentration ($\gamma = 0.01\%$). For some data points, error bars are smaller than the symbols.

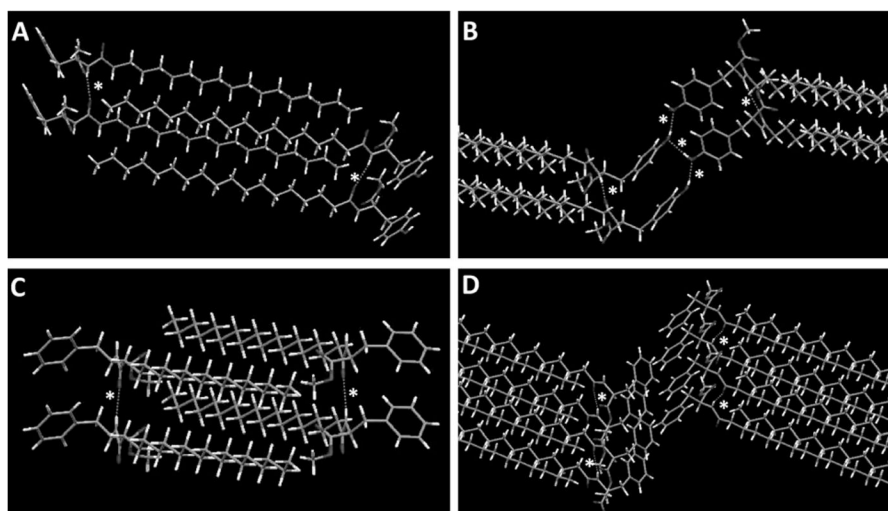


Fig. 4. Molecular packing of STyrOCH₃ (**A/B**) and SPheOCH₃ (**C/D**). Dotted lines with asterisks show H-bonds. Partial representation with 1-time lattice expansion along the b (**A/C**), b and c (**B**), and a, b, c directions (**D**).

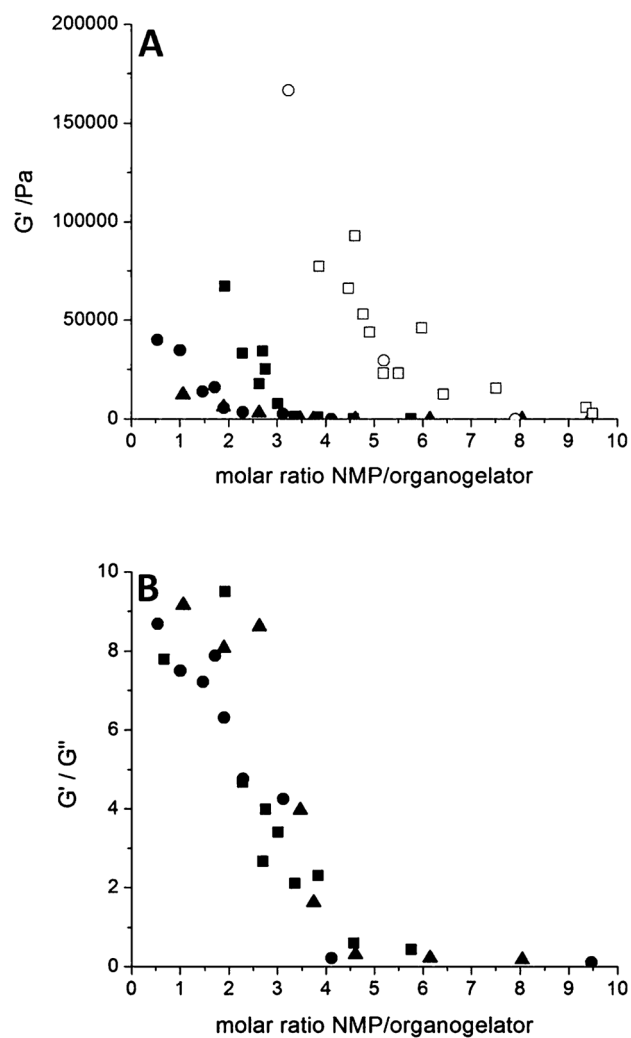


Fig. 5. (A) G' values and (B) G'/G'' ratios vs. NMP/organogelator molar ratio for formulations prepared with STyrOCH₃ at 0.2 (■), 0.1 (●) and 0.05 mmol·g⁻¹ (▲), SPheOCH₃ (□) or STrpOCH₃ (○) at 0.2 mmol·g⁻¹.

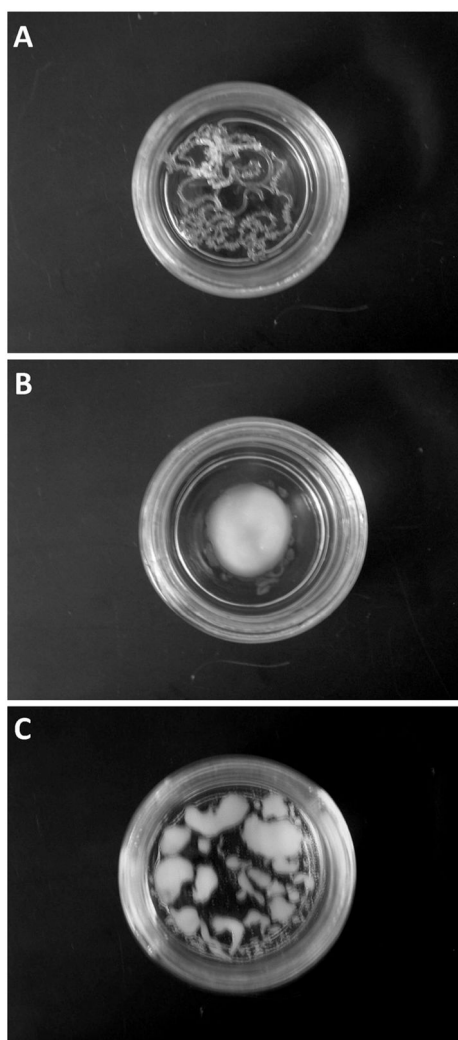


Fig. 6. Pictures of STyrOCH₃ organogels prepared with NMP after extrusion in PBS. Organogelator concentration was set at 0.2 mmol·g⁻¹ and NMP/organogelator molar ratios were 1 (**A**), 3 (**B**) and 10 (**C**).

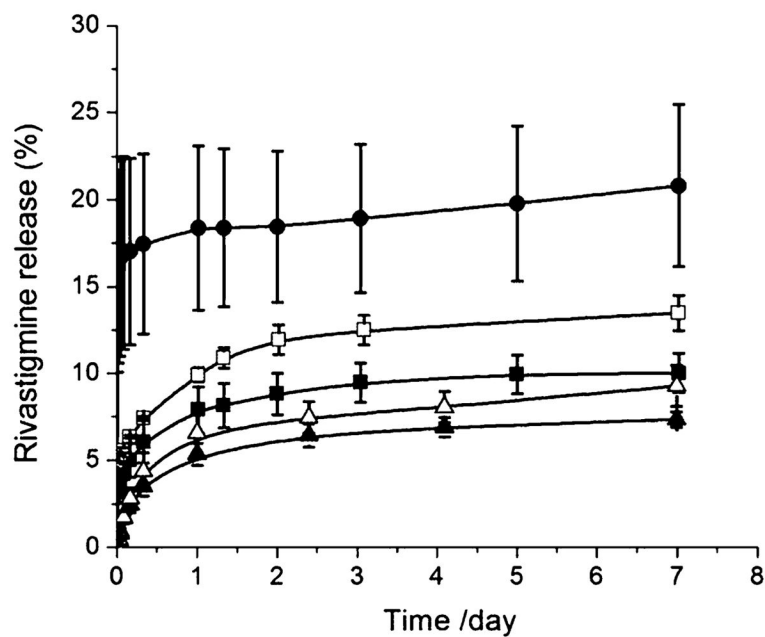


Fig. 7. *In vitro* release of RHT (3% *w/w*) in PBS at 37 °C from Tyr-based gel formulations (300 μ L): BTyrOCH₃, 0.1 (\blacktriangle) and 0.05 mmol·g⁻¹ (\triangle); STyrOCH₃, 0.1 (\blacksquare) and 0.05 mmol·g⁻¹ (\square), all with a NMP/organogelator molar ratio of 3, and STyrOCH₃, 0.05 mmol·g⁻¹ (\bullet), with a NMP/organogelator molar ratio of 6. Mean \pm SEM (n = 3).

Table 1

Enthalpy values (ΔH) of transition in the bulk and gel states obtained by DSC, and G'/G'' values of gels prepared with 0.25 mmol g⁻¹ organogelator obtained by rheology. Mean \pm SD (n = 3)^a

Organogelator	DSC		Rheology G'/G'' ($C_{\text{org}} = 0.25 \text{ mmol}\cdot\text{g}^{-1}$)
	$\Delta H/\text{kJ}\cdot\text{mol}^{-1}$ Bulk state	$\Delta H/\text{kJ}\cdot\text{mol}^{-1}$ Gel state	
SPheOCH ₃	76.1 \pm 0.1	52.4 \pm 1.0	4.3 \pm 1.3
STyrOCH ₃	56.3 \pm 1.1	60.7 \pm 0.6	8.4 \pm 1.6
STrpOCH ₃	28.9 \pm 1.1	22.8 \pm 0.6	4.3 \pm 0.9
LPheOCH ₃	38.0 \pm 3.3	17.6 \pm 9.7	n. d.
LTyrOCH ₃	36.5 \pm 2.0	36.0 \pm 4.3	n. d.
BPheOCH ₃	81.8 \pm 0.8	59.5 \pm 4.1	4.5 \pm 0.9
BTyrOCH ₃	78.7 \pm 0.8	72.3 \pm 2.9	7.7 \pm 1.8
SPheOH	40.8 \pm 2.8	32.2 \pm 4.9	n. d.
STyrOH	35.5 \pm 2.0	18.5 \pm 1.7	n. d.

^a n.d.: not determined.

Table 2

Positions of characteristic IR bands of the organogelators in solid state, gel state in safflower oil and chloroform solution^{a, b}

Organogelator	Sample state	sv OH/cm ⁻¹	sv NH amine/cm ⁻¹	sv NH amide/cm ⁻¹	sv CO ester/cm ⁻¹	sv CO amide/cm ⁻¹	bv NH amide/cm ⁻¹
SPheOCH ₃	Bulk		3338		1752	1647	1528
	Gel		3338		n. d.	1648	1530
	Solution		3432		1742	1671	1507
STrpOCH ₃	Bulk		3367	3339	1723	1639	1533
	Gel		3394	3302	n. d.	1647	1546
	Solution		3480	3430	1741	1669	1512
STyrOCH ₃	Bulk	3381		3328	1750	1645	1529
	Gel	3381		3330	n. d.	1646	1537
	Solution	3684		3431	1740	1669	1515

^a n.d.: not determined.

^b sv and bv: stretching and bending vibrations.

Table 3

Bond lengths and angles related to H-bonding in STyrOCH₃ and SPheOCH₃ crystals. Asterisks show the symmetry transformations used to generate equivalent atoms (x, y and z correspond to the a, b and c axes, respectively)

Organogelator	Donor D-H	Acceptor...A	d(D-H)/Å	d(H...A)/Å	d(D...A)/Å	D-H...A/°
STyrOCH ₃	NH (amide)	CO (amide) ^a	0.88	2.20	3.06	165.1
	N(11)-H(11)	O(12)				
	Ph-OH	Phe-O ^b	0.84	1.97	2.78	164.8
SPheOCH ₃	O(8)-H(8)	O(8)				
	NH (amide)	CO (amide) ^a	0.88	2.20	3.06	166.1
	N(11)-H(11)	O(12)				

^a x, y - 1, z.

^b -x + 1, y + 1/2, -z + 2.